Al-Qadisiyah Journal of Pure Science

ISSN(Printed): 1997-2490 ISSN(Online): 2411-3514

DOI: 10.29350/jops

Al-Qadisiyah Journal of Pure Science

Nuclear matter density distributions and elastic electron scattering form factors of one-proton halo nuclei (^{9}C, ^{12}N, ^{23}Al) within a two-parameter Folding model

Lubna Abduljabbar Mahmood

Supervision and Scientific Evaluation Apparatus, Ministry of Higher Education and Scientific Research, IRAQ

Corresponding Author: Lubna Abduljabbar Mahmood, Lubna917@yahoo.com

Abstract

This study examines the distributions of the elastic electron-scattering form factors, the nuclear matter density, and the root-mean-square radii for the nuclei with a high proton content: 9C, 12N, and 23Al. Using the Folding model with effective two-body interactions, we assess Pauli-pairing and the mass center impacts on the density. This method allows us to derive a two-body density distribution formula For selected nuclei via the pair correlation function. The nucleon density distribution for two oscillating harmonic particles, modeled by a two-frequency shell approach, uses two parameters: (bc) for core orbits and (bv) for halo orbits. Results confirm the presence of proton halo structures in 9C, 12N, and 23Al. The valence-proton configuration is pure (1p1/2) for 9C and 12N and pure (2s1/2) for 23Al. Calculated neutron and matter density distributions exhibit a significant long-tail effect, and the results align with experimental data.

Keywords: Matter density distributions, folding model, one–proton halo nuclei, root-mean square radii

1. Introduction

In modern nuclear physics, the exploration of exotic nuclei represents one of the most active research frontiers. Such studies are essential not only for revealing unconventional features of nuclear structure but also for improving our understanding of astrophysical nucleon synthesis mechanisms. The nucleus can be divided into two types: stable nuclei, which can exist in nature, and unstable nuclei (radioactive nuclei), which decay to stable nuclei within a finite lifetime. Exotic nuclei are among the most fascinating areas of study in contemporary nuclear physics because it is still unknown how many unstable nuclei exist and how they decay. The nuclear structures and behaviors of nuclei at the proton or neutron drip lines can be highly odd, posing challenges to our conventional wisdom based on experience with nuclei at or near stability (zhou, 2017). Nuclear physics is particularly interested in tensor interactions. It is essential to describe the deuteron's properties. It is important for nuclear structure, especially in exotic nuclei with extreme proton-to-neutron ratios far from stability (Dellagiacoma, et al., 1983).

A series of experiments (Nilsson T. et al.,1996) (Anne R. et al., 1990) has been conducted to investigate protons and neutrons in structurally well-defined, proton-rich or neutron-rich nuclei. In nuclear physics, an exotic nucleus is a configuration in which a secondary cluster of protons orbits the central core, with the majority of the nucleus enveloped by this cluster. These protons have very short lifetimes; at the same time, the energy needed to remove the outer cluster from the nucleus near the drip line is minimal. Several approaches have been developed to address the influence of tensor forces on the ground-state properties of nuclei (Bethe et al., 1963) (Kuo and Brown, 1967). Providencia and Shakin (1964) utilized a nearest-neighbor correlation operator to describe short-range correlation effects, similar to the method employed by Pacchi and Milecki (1968).

To introduce dynamical and tensor correlations, Dellagiacoma et al. 1983 devised a simple phenomenological method. One-proton halo 17F nuclei were used to calculate double-folding potentials using two different density models. The characteristics of exotic nuclei and how they relate to nucleonic interactions (Nakada, 2020). (Luay et al., 2020) studied the densities of 14B and 17C using the cluster model (BCM).

A different study employed a similar approach to examine the properties of the exotic nuclei 18N and 20F, using a two-body model with Gaussian and Woods-Saxon wave functions. The calculations successfully captured the characteristic long-tail density distributions and revealed significant differences in elastic form factors (calculated via PWBA) compared to their stable isotopes (14N and 19F) due to valence neutron effects (Hawraa et al., 2022). investigation into the nuclear structure of halo nuclei 23O and 24F utilizing a two-body model of (core + n) within Woods-Saxon radial wave functions and harmonic oscillator that, conducted b (Ghufran et al., 2020).

The goal of this study is to develop distributions of the two-body density relevant to limit nuclei, accounting for center-of-mass and Pauli-pair association effects that depend on effective two-body interactions relative to the pair correlation function. the formula depending on the folding model and considering the nuclei to be made of more one part, the nucleus with the halo, for the nucleus (^{22}N, ^{23}O and ^{24}F) is studied taking into account the nuclei (core + p) and calculated of form factors and rms radii which depending on TBCDD formula and the pauli pair and center of mass correlations function of the neutron-rich halo nuclei. The function of the pair correlation is to determine the equation for the two-body operator density within the folding model.

2. Theory

The operator did the nucleon density of a nuclei (contain *A* particles with point shape) (Ghufran et al., 2020) study of the nuclear structure of halo nuclei 23O and 24F using the two-body model".

$$\rho^{(1)}(\mathrm{r}) = \frac{1}{4\pi}\sum_{n\ell j}\eta_{n\ell j}.2.(2j+1)\left|R_{n\ell}(\mathrm{r})\right|^2$$

(1)

where the parameter $\eta_{n\ell j}$ is the occupation percentage of $n\ell j$. Hence $\eta_{n\ell j}$=0 or 1 for closed shell nuclei, while for open shell nuclei , we use the same expression of eq (1) but now $0 < \eta_{n\ell j} < 1$. $R_{n\ell}(\mathrm{r})$ is function of the harmonic oscillator radial wave that base on parameters of the harmonic oscillator size (*b*)

The folding model provides an effective framework for analyzing nucleon-nucleus scattering outcomes by utilizing the target's ground-state density and a two-body effective interaction (Ahmad, 1995). Initial implementations of this model treated the target density as independent of the effective interaction. The pair correlation function enables the equation derivation for the two-body operators density used to finite nuclei, as demonstrated below:

$$\rho^{2}(\vec{r}_1,\vec{r}_2) = \rho^{(1)}(r_1)\ \rho^{(2)}(r_2) + C(\vec{r}_1,\vec{r}_2)$$
(2)

$C(\vec{r}_1,\vec{r}_2)$ is mass center (*c.m.*) and Pauli pair C_{cm} and C_p, respectively (AHMAD et al., 1981), so that

$$C(\vec{r}_1,\vec{r}_2) \cong C_{c.m.}(\vec{r}_1,\vec{r}_2) + C_p(\vec{r}_1,\vec{r}_2)$$
(3)

Where :

$$C_{c.m.}(\vec{r}_1,\vec{r}_2) = \frac{r_1.r_2}{2A\alpha^2}\left(\frac{1}{r_1}\frac{d\rho_1}{dr_1}\right)\left(\frac{1}{r_2}\frac{d\rho_1}{dr_1}\right)$$
(4)

$$C_p(\vec{r}_1,\vec{r}_2) \cong \frac{1}{A-1}\left[1 - \frac{c_o}{A-1}e^{\frac{k_f^2}{5}|\vec{r}_1-\vec{r}_2|}\right]\rho^{(1)}(\vec{r}_1)\rho^{(1)}(\vec{r}_2)$$
(5)

Substitute equations (4) and (5) into (3) and using equation (3) in equation.(2), we get:

$$\rho^{(2)}(\vec{r}1,\vec{r}2) = \rho^{(1)}(\vec{r}1)\rho^{(1)}(\vec{r}2) + \frac{r_1.r_2}{2A\alpha^2}\left(\frac{1}{r_1}\frac{d\rho_1}{dr_1}\right)\left(\frac{1}{r_2}\frac{d\rho_1}{dr_1}\right) + \frac{1}{A-1}\left[1 - \frac{c_o}{A-1}e^{\frac{k_f^2}{5}|\vec{r}1-\vec{r}2|}\right]\rho^{(1)}(\vec{r}_1)\rho^{(1)}(\vec{r}_2) \quad (6)$$

where $c_0=3(\pi/5)^{1/2}$, α is the oscillator constant $\left(\alpha^2 = 0.99\,A^{-1/3}\right)$ and K_f is local Fermi momentum.

The result provided distribution of the state two-body for the distribution of the functional two-body of the charge density (6) as:

$$\rho^{(2)}(r) = \sum_{i<j}\langle i\,j|\rho^{(2)}_{(r_i,r_j)}[|i\,j\rangle - |j\,i\rangle]$$
(7)

where $|ij\rangle$ the wave function for two particles. In the scenario of halo nuclei, it is reasonable to treat the core and halo densities independently. The way in which the ground-state matter density distribution of exotic nuclei is defined is given in reference (Abdullah, 2020).

$$\rho_m(r) = \rho^{core}_{(p+n)}(r) + \rho^{valence}_n(r)$$
(8)

The root mean square radii for the respective densities mentioned above are provided by (Antonov et al., 2004).

$$\langle r^2\rangle_u^{1/2} = \frac{4\pi}{u}\int_0^\infty \rho^u(r)r^4\,dr$$
(9)

Where *u* is (proton, neutron or matter).

The form factors for elastic electron scattering are emitted by the nuclei being examined (Brown et al., 1983).

$$F(q) = \frac{4\pi}{qZ}\int_0^\infty \rho_o(\mathrm{r})\,Sin(q\mathrm{r})\mathrm{r}\ d\mathrm{r}\,F_{fs}(q)\,F_{cm}(q)$$
(10)

Where the nucleon finite correction for size $F_{fs}(q)$ is defined [Brown et al., 1983] :

$$F_{fs}(q) = e^{-0.43 q^2/4}$$
(11)

Within this framework, the free nucleon form factor Ffs (q) is considered identical for neutrons and protons. Mass correction center Fcm (q) as (Walecka, 2001).

$$F_{cm}(q) = e^{q^2 b^2/4A}$$
(12)

Here, A denotes the number of the nuclear mass, and b is the parameter of the harmonic-oscillator size.

3. Results and Discussion

The distributions of matter density for one-proton halo nuclei in their ground states (9C, 12N, 23Al) and the root mean square radii associated with the form factors testing by the two-body harmonic oscillator model, with (bc) and (bv).

The folding model, designed to reveal how the center of mass and Pauli-pair associations influence nuclear density, can be captured by a formula for the two-body density of limit nuclei in terms of the pair-correlation function. By applying this approach, the ground-state properties of halo nuclei were uncovered through the two-body density, as detailed in equations (Kuo and Brown, 1967) (Providencia and shakin, 1964) (Malecki and Picchi,1968). Table 1 showcases key features of halo nuclei (Ozawa et al., 2001) (Warner et al., 2006) (Zhao et al., 2003)(Zhang et al., 2005). The characteristic radii of neutrons and protons, determined through equations 9 and 8, are also highlighted in the table.

In Table 1, the βc and βv values from the TFSM are presented, along with the observed and calculated rms radii for 9C, 12N, and 23Al.

Halo nuclei	Core nuclei	*bc* (fm)	*bv* (fm)	rms matter radii for $\langle r^2\rangle^{1/2}_{core}$ (fm)	
				Calculated	Experimental
^{9}C	^{8}B	1.85	2.10	2.44	2.38±0.04 [21]
^{12}N	11C	1.62	1.80	2.28	2.18 ±0.26 [22]
^{23}Al	^{22}Mg	1.88	1.97	2.85	2.78± 0.26 [23]

1. 9C Nucleus

The nucleus 9C is generated by compine 8B core with a valence proton. An oscillator size parameter for the 8B core (bc = 1.85 fm) yields a root-mean-square (rms) nucleon radius of 2.44 fm. For the valence proton in the exotic nucleus 9C, a pure configuration (1p1/2) with oscillator size parameter (bv) of 2.10 and occupation probability (0.25) fm, findings in rms nucleon radius of 2.77 fm, which is detected by the matter density distribution, and that agrees with table 1. Figure 1 presents the variation of matter density as a function of distance r (fm). In Figure 1-a, the black line represents the contribution from the core 8B, while the blue line, corresponding to the valence component, exhibits a pronounced long tail. The total matter density, depicted in red, also shows an extended tail and closely aligns with the 9C data from Hong et al. (2005), shown as filled circles. Figure 1-b provides a comparison between the matter density distributions of the stable 12C nucleus and the 9C nucleus.

line).

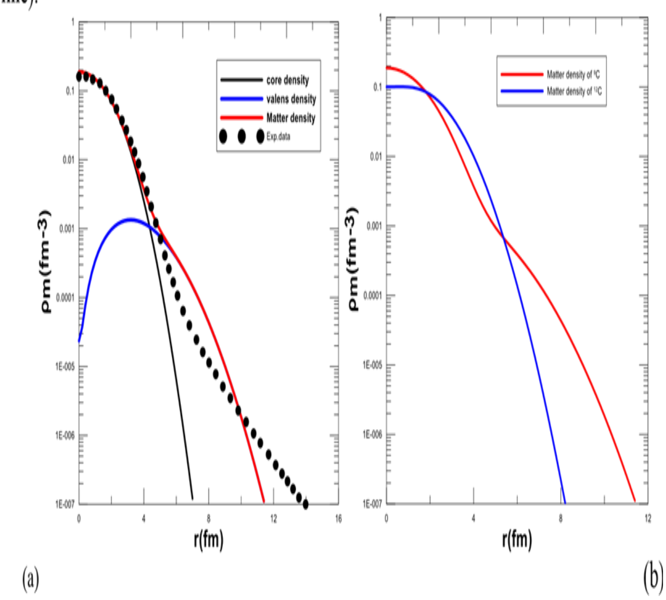

Figure 1- (a) A comparison between the distribution of the matter density and the data for 9C. (b) Comparison of the matter density of 9C with nucleus 12C.

Figure 2 presents the elastic electron-scattering form factors; the red line is obtained using the oscillator size b = 1.9 fm. The filled circle is the particle data for 12C (Crannell, 1966). 9C shows behavior comparable to 12C; the first diffraction minimum is at -1 for 9C and at -1 for 12C.

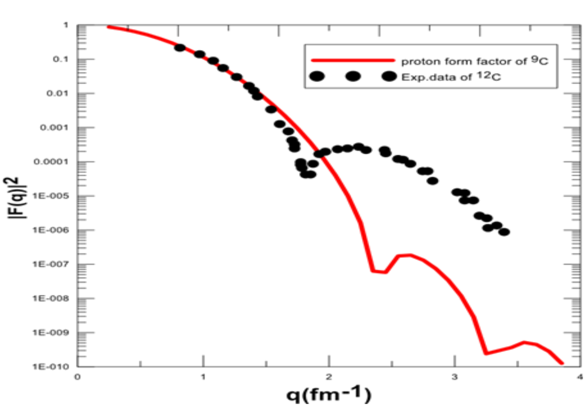

Figure 2- highlights the differences in elastic electron scattering form factors between 9C and 12C, offering a clear comparison based on data from (Brown and Radhi, 1983).

2. 12N Nucleus

The nucleus 12N is formed by combining the core nucleus 11C with an additional proton in its valence shell. Parameter of the oscillator size for 11C core is βc = 1.62 fm, resulting in rms of 2.28 fm. The valence proton forms a pure 1p1/2 state with parameters of the oscillator size of βv = 1.70 fm, occupation number of 0.25, and rms radius of 2.57 fm. rms radii were provided from the distribution of the matter density as Table 1. Distribution of the matter density (Figure 3).

The black line in Figure 3(a) is 11C core contribution, while the blue line corresponds to the valence proton, leading to a distribution with an extended tail. The red line shows the entire matter density distribution, which has a long tail, in agreement with Xing et al. (2010). The filled circle. Figure 3(b) compares the red and blue lines.

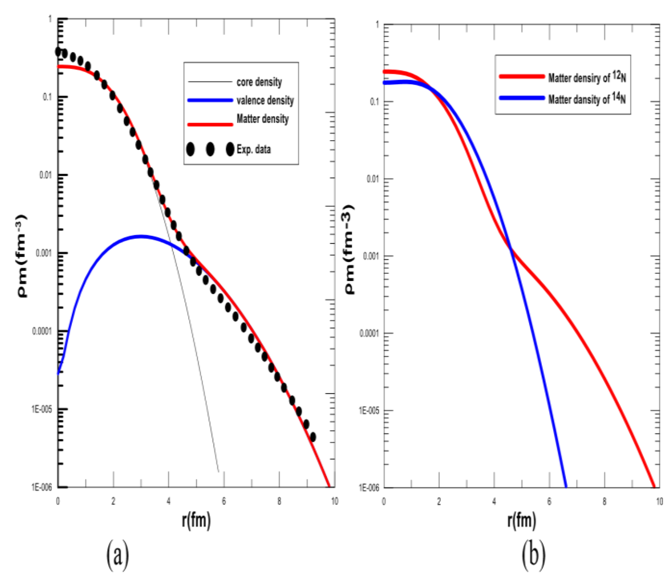

Figure 3- (a) Comparison between the distribution of the matter density and experimental data for ^{12}N .(b) Comparison between ^{12}N nuclei and ^{14}N density.

The elastic electron-scattering factors are shown in Figure 4, where the red line corresponds to factors with an oscillator size parameter β = 1.71 fm (βc and βv). The filled circle symbol shows 12N (Dally et al., 1970). When comparing, they exhibit a trend to the experimental data for 14N; however, the first diffraction minimum for 12N occurred at -1, whereas for 14N it was at

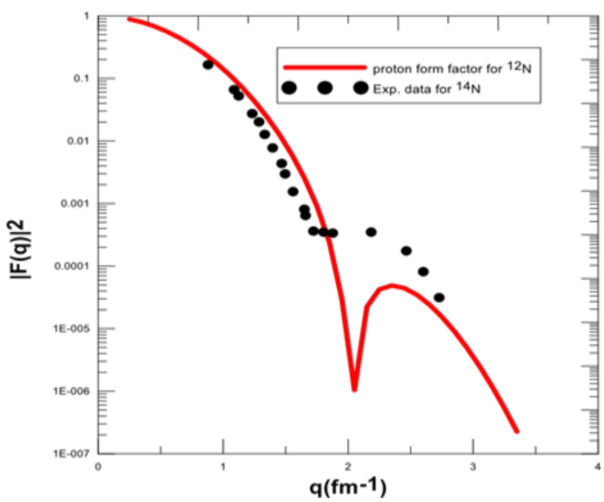

Figure 4- Comparison between ^{12}N and experimental data of ^{14}N in elastic electron scattering

3. 23Al Nucleus

The nucleus 23Al is created by combining the core nucleus 22Mg with an additional proton. Parameters of the oscillator size for 22Mg is (βc=1.88fm), resulting in rms radius of (2.85fm). At the same time, the valence proton forms the pure (2s1/2) state with an occupation number of 0.25 and parameters of the oscillator size βv of 1.97fm, leading to an rms radius of (2.98fm) that was detected by the distribution of the matter density. In addition, the findings agree with the experimental data.

The black line in Figure (5-a) represents the contribution of core 22Mg, while the blue line illustrates the valence, which features an extended tail. Distribution of the matter density combining the valence and the core, wherever the red line represents the long tail and aligns well with (Fang et al., 2005). Figure (5-b) compares the distribution of the density of 34Al

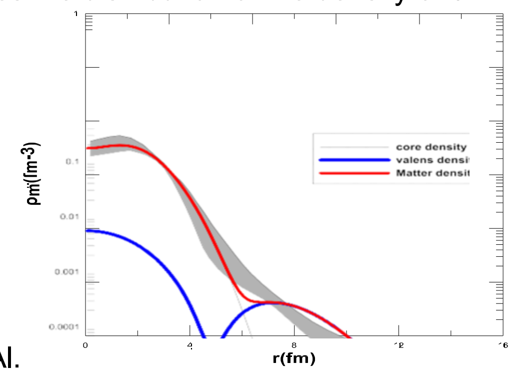

and 27Al.

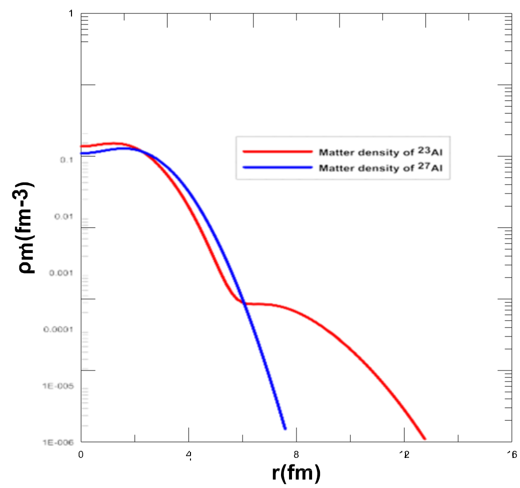

(a) (b)

Figure 5-(a) illustrates a comparison of disterbution of the the matter density of 23Al with the experimental data. (b): compared between 23Al nuclei with 27Al matter density.

Figure 6 presents the elastic electron scattering form factors. The red line shows the form factors for the oscillator size parameter β=1.93 fm. The filled circle shows the experimental findings for 23Al (Li and Yearian, 1974), which are compared with the theoretical findings for the elastic scattering of 23Al and the practical findings for 27Al. The first diffraction minimum is shown at q = 1.6 and 1.5 fm-1 for 23Al and 27Al, respectively.

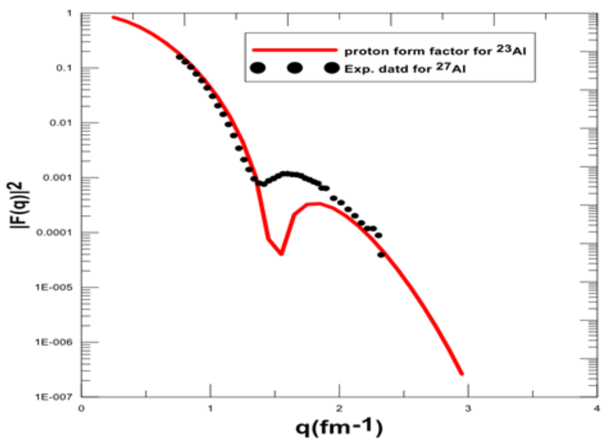

Figure 6 - A comparison of elastic electron scattering form factors with the experimental data for 27Al, highlighting key similarities and differences [27]

4. Conclusion

While proton valence is often highlighted as a hallmark of halo nuclei, this study turns its attention to those with neutron valence. On the other hand, the neutron halo formed a 2s1/2 orbital. At the same time, the calculated matter density for these nuclei revealed a pronounced tail, captured by the distribution of the two-nucleon density within a folding model for parameters of the core and valence oscillator sizes, bcore and bvalence. These findings closely matched experimental findings. The striking contrast in form factors between stable counterparts (12C, 14N, and 27Al) and unstable nuclei (9C, 12N, and 23Al) can be traced to the unique charge distribution of the neutrons.

References:

Abdullah A. N., Int. J. Mod. Phys. E 29, 2050015 (2020).

AHMAD I. , J.P. AUGER , Nuclear Physics A352 (1981) 425-441 ,North-Holland Publishing Co., Amsterdam

Ahmad I., "Folding model with three-body force," Journal of Physics G: Nuclear and Particle Physics, 20, 3, 507, 1994.

Ahmed N. Abdullah, "The neutron halo structure of 14B, 22N, 23O and 24F nuclei studied via the generalised Woods–Saxon potential". Pramana – J. Phys. (2020)94:154.

Anne R. et al., Phys. Lett. B 250,19 (1990).

Antonov A.N., Gaidarov . K., Kadrev D.N., Hodgson P. E. and Guerr E. M. D., Int. J. Mod. Phys. E 13, 759 (2004).

Bethe H., B. H. Brandow and. A. G. Petschek (Reference spectrum method for nuclear matter), Phys.Rev., 129, 1, 1963, 225-264.

Brown B. A. , Radhi R. A. and Wildenthal B. H ; Physics Report, 101,313 (1983).

Crannell, H. "Elastic and Inelastic Electron Scattering from C12 and O16". *Phys. Rev.*148:1107,1966.

Dally E. B. Croissiaux M. G. and Schweitz. B."Scattering of High-Energy Electrons by Nitrogen-14 and -15", *Phys. Rev*. C 2: 2057,1970.

Dellagiacoma, F., Orlandini, G. and Traini, M. , Nuclear Physics A, 393,(1983).

Dellagiacoma, F., Orlandini, G. and Traini, M. , Nuclear Physics A, 393,(1983).

Fang D. Q. Wang M. C. Gang M. Y. , Zhou C. X. , Gen, C. J. Hui, G. Wei, T. Dong, W. Kun, W. Bin, Y. T. Zhi, Z. Chen, Z. J. Xu, S. W. Qing, *Chin. Phys*. Lett. 22 , 572,2005.

Ghufran M. Sallh, Ahmed N. Abdullah . Iraqi Journal of Physics, 2020 Vol.18, No.46, PP. 29-38." Study of the nuclear structure of halo nuclei 23O and 24F using the two-body model".

Hawraa K. Mahdi and Ahmed N. Abdullah, “Elastic Form Factors and Matter Density Distributions of Some Neutron-Rich Nuclei,” Iraqi Journal of Physics, vol. 20, no. 4, pp. 18–27,2022.

Hong L.Z., Bing G., Ping L. W., Xiang B. X., Gang L , Jun S, Quan Y. S., Xiang W. B and Sheng Z, *Chin. Phys*. Lett. 22 :1870,2005.

Kuo T. T. S. and Brown G. E.,"Structure of finite nuclei and the free nucleon-nucleon interaction", Nucl. Phys., A92, 3, 1967, 481-494.

Li G. C., Yearian M. R. and Sick I., "High-momentum-transfer electron scattering from ^{24}Mg, ^{27}Al, ^{28}Si, and ^{32}S", *Phys. Rev*. C 9 :1861,1974.

Luay F. Sultan and Ahmed N. Abdullah . Al-Nahrain Journal of Science ANJS. 23,(2020).

Maha Taha Yaseen , Akram M. Ali," Charge Density Distributions, Momentum Density Distribution, and Elastic Form Factors of Exotic One- And Two-Proton Halo Nuclei " Journal of critical reviews, ISSN- 2394-5125 Vol 7, ISSUE 15, 2020.

Malecki A. and Picchi P.,"Elastic electron scattering from4He", Phys. Rev. Lett., 21, 19, 1968, 1395-1398.

Nakada H., International Journal of Modern Physics E 29, (2020) .

Nilsson T. et al., Nucl. Phys. A 598, 418 (1996).

Ozawa A. , Suzuki T., Tanihata I, "Nuclear size and related topics", *Nuclear Physics* A 693(1-2), :32-62,2001.

Providencia J. Da and shakin C. M., "Some aspects of short-range correlation in nuclei", Ann. Phys., 30, 1, 1964, 95-118.

Walecka, J. D. (Electron Scattering for Nuclear and Nucleon Structure), Cambridge University Press, Cambridge, 2001, 14-16.

Warner R. E., Carstoiu F. Brown J. A., Becchetti f. D. , Roberts D. A. Davids B., Galonsky A., Ronningen R. M., Steiner M. Horoi M., Kolata J., A. Nadasen A., Samanta C., Schwartzenberg J. and Subotic K., "Reaction and proton-removal cross sections of ^{6}Li, ^{7}Be, ^{10}B, ^{9,10,11}C, ^{12}N, ^{13,15}O, and ^{17}Ne on Si at 15 to 53 MeV/nucleon", *Phys. Rev*.C 74: 014605,2006.

Xing L. J., Ping L. P., Song W. J., Guo H. Z., Shi M. R., Yu S. Z., Chen I., Fu c. r., Shan X. H. , Qing X.G. and Yan G. Z. *, Chinese Physics* C 34 : 452,2010.

Zhang H.Y., Shen W.Q. Ren, Z.Z., Ma Y.G., Jiang W.Z., Zhu Z. Y., Cai, X. Z. Fang D. Q., Zhong C., Yu L.P., Wei Y.B., Zhan W.L., *Chin Phys*.Lett.22:3,2005.

Zhao Y. L., Yu M. Z., Qiu C. B. and Qing S. W. , *Chin. Phys*. Lett. C 20 : 53,2003.

zhou S.-G., “Structure of Exotic Nuclei: A Theoretical Review,” 2017